Nuclear wave-packet dynamics on nearly degenerate two adiabatic potential energy surfaces in the excited state of KI *F* centers

Takeshi Koyama, Youtarou Takahashi, Makoto Nakajima, and Tohru Suemoto
Institute for Solid State Physics, The University of Tokyo, Kashiwanoha 5-1-5, Kashiwa-shi, Chiba 277-8581, Japan
(Received 8 March 2007; revised manuscript received 17 July 2007; published 20 September 2007)

Nuclear wave-packet dynamics in the excited state of KI *F* centers is investigated by using time-resolved luminescence spectroscopy based on the up-conversion technique. The observed transient spectrum involves an oscillatory and a nonoscillatory component. The origins of these components are interrogated by comparing the results with a model calculation based on the resonant secondary radiation theory. The oscillatory part reflects the coupling of the 2*s*-like electron mainly to the totally symmetric local mode around the *F* center. The nonoscillatory part reflects the incoherent population of the vibrational levels in the 2*p*-like state, which couples to many bulk phonon modes with a broad density of state. The model calculation suggests that the transition probability to the 2*p*-like state is approximately 0.05.

DOI: 10.1103/PhysRevB.76.115122 PACS number(s): 78.47.+p, 61.72.Ji, 63.20.Kr, 63.20.Pw

I. INTRODUCTION

Ultrafast dynamics of atoms or molecules in solids is an important issue for understanding and controlling chemical processes,[1] defect formations,[2] and photoinduced phase transitions.[3,4] Coherent lattice motions are expected to play a key role in promoting such phenomena at their intermediate states. The coherent lattice vibrations in macroscopic scale is termed as the coherent phonons,[5] which behave as a classical mechanical wave. They reflect the bulk vibrational spectrum under moderate photoexcitation conditions, while in the case of high density excitation, anharmonic phonons appear.[6,7] By contrast, the coherent atomic motions in localized systems are suitably understood by the concept of the nuclear wave packet (NWP). The NWP is a coherent superposition of several vibrational sublevels on the adiabatic potential energy surface (APES) and is considered as a quantum mechanical wave.

The local lattice vibration is described in terms of the interaction mode,[8,9] i.e., the linear combination of a number of normal modes consisting of bulk phonon modes as well as local modes. The coupling of normal modes to a localized electron depends on the size and the symmetry of the relevant electronic wave function.

Recently, we have investigated the excited *F* center in a KI crystal through time-resolved luminescence spectroscopy. The experimental results suggest that a portion of the NWP diabatically transfers to the upper-lying nearly degenerate APES.[10] In the present paper, we perform a model calculation for the temporal evolution of the luminescence spectrum and quantitatively interrogate the NWP dynamics in the excited state of the *F* center.

The *F* center in alkali halides is a prototype of a strongly coupled localized electron-phonon system, which consists of an anion vacancy occupied by a single electron. Its configuration coordinate diagram is illustrated in Fig. 1(a). The excited state is composed of nearly degenerate 2*s* and 2*p* states. The Stark effect experiments show that the 2*s* state lies above the 2*p* states in the Franck-Condon state (FCS) of absorption around a hundred meV (90 meV in KI *F* centers),[11] but is lower in the relaxed excited state (RES) about several tens of meV (41.17 meV in KI *F* centers).[12] The RES is called the 2*s*-like state because it is described as the 2*s* state admixed with a part of upper-lying 2*p* states via the pseudo-Jahn-Teller effect due to the T_{1u} phonon modes.[13] Above the 2*s*-like state lies the 2*p*-like state, which is described as the 2*p* states admixed with a part of the 2*s* state. In contrast, the FCS has a character of nearly pure 2*p* states. The Stark effect experiments show that the 2*s* and 2*p* levels cross each other between the FCS and the RES. Recently, Akiyama and Muramatsu have indicated that the relaxation proceeds from the 2*p* state to the 2*s*-like state through an anticrossing region.[14]

The optical process at the *F* center has been understood as follows. Optical absorption excites the system adiabatically from the 1*s* ground state to the FCS with a NWP created on the 2*p* APES [Fig. 1(b)]. The lattice starts to expand to the new equilibrium point; i.e., the NWP starts to move toward

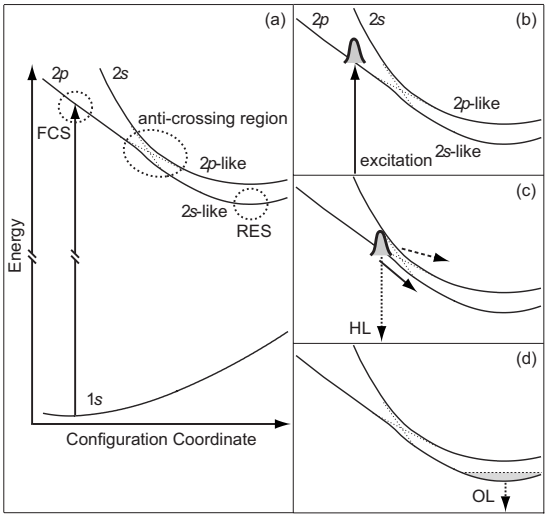

FIG. 1. Schematic drawings of the excited-state dynamics at the *F* center in the configuration coordinate space. (a) Configuration coordinate diagram. [(b)–(d)] Nuclear wave-packet dynamics in a sequence of optical processes from absorption to ordinary luminescence (see text).

 ©2007 The American Physical Society

the potential minimum in the excited state. The NWP propagates from the $2p$ state to the $2s$-like state almost continuously through the anticrossing region along the lower APES [solid arrow in Fig. 1(c)]. Then, it oscillates around the potential minimum. After the NWP motion is damped and the thermalized population is established, the system returns to the ground state by emitting a photon [Fig. 1(d)]. This emission is so-called ordinary luminescence (OL), whose decay time is several microseconds (e.g., 2.22 μs for the F center in KI at 10 K).[15] Even though the vibrational relaxation proceeds so fast, some centers emit photons before thermalization; this emission is called hot luminescence (HL). The instantaneous shape of the NWP on the APES can be captured through the transient luminescence spectrum.

Although the NWP passes through the anticrossing region almost adiabatically, some portion will transfer to the upper APES diabatically [dashed arrow in Fig. 1(c)]. The HL around the potential minimum at the earlier stage of relaxation cannot be observed in stationary luminescence spectra because the HL is obscured by the OL: The time-integrated OL intensity is $\sim 10^5$ times larger than the HL.[16–18] In order to understand the NWP behavior, it is necessary to perform real-time measurements. Time-resolved spectroscopy measurements with time resolutions of picoseconds or a few hundred femtoseconds have been done for the F centers in KCl,[19–22] NaBr,[23] or NaI.[24] Ultrafast pump-and-probe experiments have been performed for KBr F centers with ~ 10 fs laser pulses under the so-called degenerate pump-probe conditions.[25,26] However, the NWP behavior around and after the anticrossing region have not been elucidated in these real-time measurements.

In order to investigate the unrevealed excited-state dynamics depicted in Fig. 1(c), we conduct the time-resolved luminescence spectroscopy for KI F centers. A model calculation of the time-resolved spectrum is also performed based on the resonant secondary radiation theory applied to the system with two excited states. The experimental results are compared with those from the calculation, and the NWP dynamics is studied.

The remainder of this paper is outlined as follows: In Sec. II, the experiment of the frequency up-conversion spectroscopy is explained. The experimental results are presented and analyzed. Section III describes the model calculation based on the resonant secondary radiation theory in the case of the strong electron-phonon coupling limit. Section IV addresses the interpretation of the experimental results by referring to the calculation results.

II. EXPERIMENT

Luminescence methods have advantages for studying the excited states at localized systems. When the luminescence photon energies are suitably selected to be far from the energy of the absorption band, obtained results are free from the ground-state dynamics.[27–33] Furthermore, the participating optical transition is only from the excited state to the ground state, so that the complication due to the higher excited states can be avoided, which often causes difficulties in analyzing data of pump-and-probe experiments.

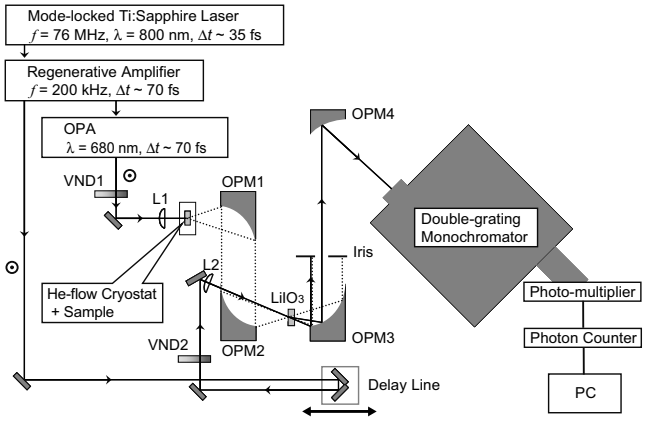

FIG. 2. Schematic diagram of the system for a transmissive up-conversion measurement. VND1, VND2, variable neutral-density filters; L1, L2, planoconvex lenses; OPM1-4, off-axis paraboloidal mirrors.

A. Experimental setup

Crystals of KI were obtained from Korth Kristalle GmbH and additively colored up to F-center concentrations of approximately 5×10^{16} cm^{-3} by van Doorn's method.[34] A schematic diagram of our system for a transmissive up-conversion measurement is drawn in Fig. 2. Cleaved samples, 300 μm thick, were mounted in a He-flow cryostat operating at 10 K. The light source was a regenerative amplifier (200 kHz, 800 nm, 70 fs), which was seeded by a mode-locked Ti:sapphire laser (76 MHz, 800 nm, 35 fs). A part of the output of the amplifier was used as a gate pulse and the rest was used to pump an optical parametric amplifier (OPA), which generated an excitation pulse. The excitation light was polarized parallel to the [100] crystal axis of KI. The average excitation power was 1 mW. The excitation photon energy was 1.823 eV, which corresponds approximately to the peak energy of the absorption band of the F center in KI; the absorption band peaks at 1.875 eV with a full width at half maximum (FWHM) of 0.155 eV at 10 K.[35] The sum frequency signal was generated by mixing the luminescence photons with the time-delayed gate pulses in a 1-mm-thick lithium iodate ($LiIO_3$) crystal with a cutting angle of 37.4°. Owing to the type-I phase matching, detected luminescence has the polarization direction parallel to that of the gate pulse, which was set parallel to that of the excitation pulse. After being collimated, the signal light was spatially and spectrally separated by an iris and a double-grating monochromator, respectively, from the remnants of the gate pulses and unphase-matched second harmonics of the gate pulses. The signal light was detected by a photomultiplier tube and a photon counter. The overall time resolution of the measurement system was 110 fs. The spectral resolution was about 0.06 eV. The spectral sensitivity of the system was measured by means of the up-conversion signal of a tungsten standard lamp. The luminescence was detected in the photon energy range 0.7–1.3 eV, involving the emission peak at 0.827 eV.[36]

B. Results and analysis

Figure 3 shows the time evolutions of luminescence intensities measured at different photon energies. The relative

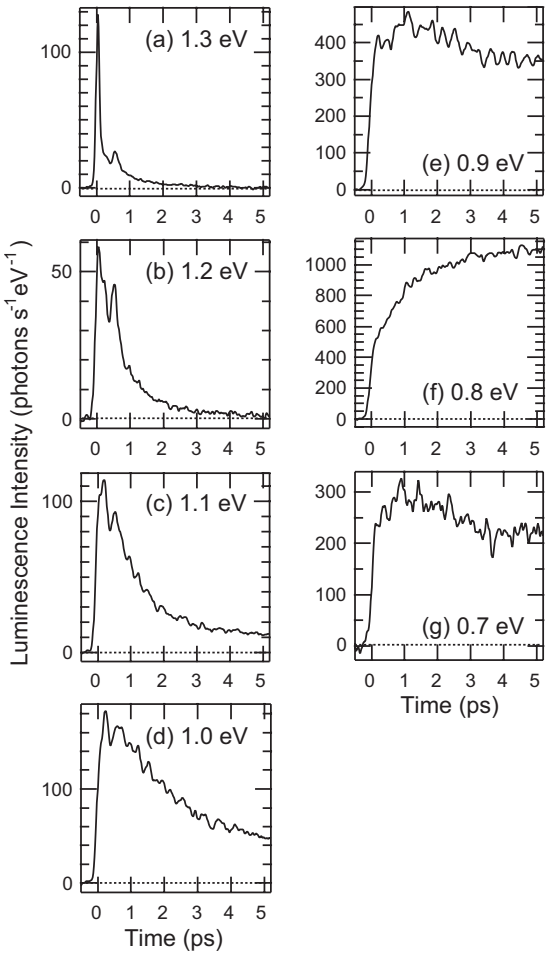

FIG. 3. Time evolutions of luminescence intensities at different photon energies. The ordinates show the calibrated luminescence intensity in the units proportional to photons per unit second per unit energy.

intensity at each photon energy is calibrated with respect to the 1.3 eV luminescence. The time origin was defined as the center point of the cross-correlation signal between the gate pulse and the excitation pulse scattered at the surface of the sample. As the luminescence experiences a 1.5-mm-thick fused silica window of the cryostat, each time origin is shifted in this figure to compensate for respective time advances due to the group velocity dispersion of this window.

In the high energy region, 1.0 eV and above [Figs. 3(a)–3(d)], the decay time becomes longer as the photon energy decreases. The 0.8 eV trace [Fig. 3(f)] indicates a fast rising within the time resolution, a kink around 0.1 ps, and a gradual rise for several picoseconds. Since the time constant of the gradual rise corresponds to that of the decay of the 1.2–1.3 eV luminescence, it reflects the concentration of the probability amplitude toward the potential minimum associated with the NWP damping. The temporal evolutions of the 0.9 and 0.7 eV luminescences in Figs. 3(e) and 3(g) resemble each other. This is in accordance with the fact that the 0.8 eV luminescence occurs near the potential minimum.

Figure 4 shows the oscillating components, which are extracted by subtracting the smoothed envelope from the traces

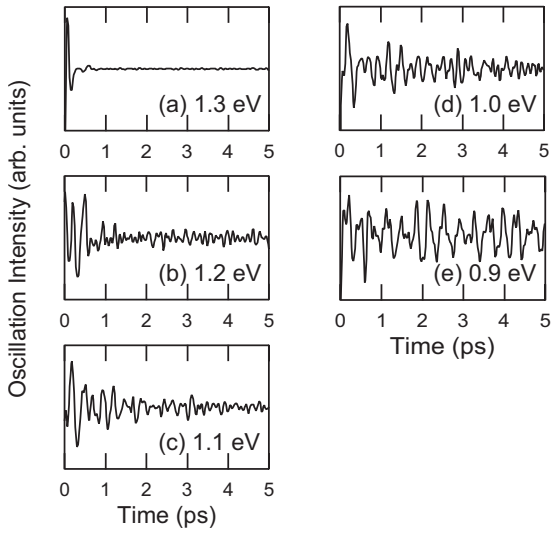

FIG. 4. Oscillating components at different photon energies.

in Fig. 3. The decay time of the oscillation decreases as the photon energy increases. The oscillation at 0.9 eV lasts over the detected time region with a steady amplitude [Fig. 4(e)]. The oscillation at 1.1 eV almost disappears by 5 ps [Fig. 4(c)]. The disappearance of oscillation indicates that after 5 ps the NWP does not reach the probe window at 1.1 eV. If the NWP does not come to the probe window, the luminescence intensity should be zero at that energy. However, Fig. 3(c) shows appreciable nonoscillatory luminescence intensity remains at 5 ps. The nonoscillatory component indicates the existence of an incoherent population. It is unlikely that the incoherent population coexists with the wave packet (coherent state) on the same APES because we have to assume different decoherence rates for the higher and lower vibrational levels for realizing such a situation. Therefore, it is conceivable that there is another luminescent state, in which the incoherent population is established by 5 ps.

In order to examine the long-lasting oscillation in the 0.9 eV wave form, the Fourier transformed spectrum of the oscillating component between 0.3 and 5.0 ps in Fig. 4(e) was calculated using the Hanning window function and is shown in Fig. 5(a). The spectrum shows the highest peak at 2.8 THz; this value is nearly equal to the frequency of the A_{1g} local mode at 2.89 THz observed in the resonance Raman spectrum.[37] In both sides of this remarkable peak, several structures are seen. Comparing them with the density of state (DOS) of bulk phonons in KI,[38] the structures at the low frequency side are attributed to acoustic phonon modes near zone boundaries and singularity points, and those at the high frequency side to optical phonon modes.[39] Bulk phonon modes have been observed for other localized systems, e.g., the F center in KBr (Ref. 32) and dihalogen-doped rare gas crystals (Refs. 40–42).

III. CALCULATION

In this section, we describe the model calculation of the time evolution of the luminescence spectrum. The calcula-

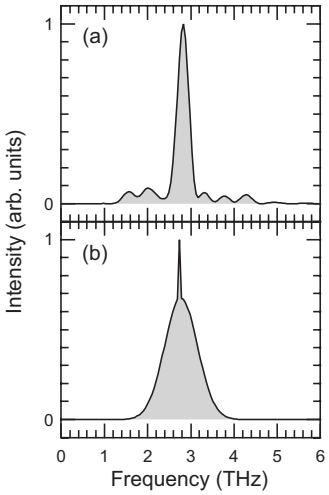

FIG. 5. (a) Fourier power spectrum of the oscillatory component extracted from the luminescence intensity at 0.9 eV. (b) Spectral density function used in the calculation for the hot luminescence from the 2*s*-like state.

tion is performed based on the resonant secondary radiation theory in the strongly coupled localized electron-phonon system.

Resonant secondary radiation theory describes a sequence of optical processes at localized electron-phonon systems from resonance Raman scattering over HL to OL. The theory has been developed by Hizhnyakov and Tehver,[43,44] Toyozawa,[45] and Toyozawa *et al.*[46] Then, it has been applied to the calculation of the NWP dynamics in the strong electron-phonon coupling case.[47–50] We proceed along the time-dependent formalism of Ref. 50.

Several calculations of the resonant secondary radiation at optical centers have been performed mainly for the two-level system with the electron-phonon coupling. In order to describe the case of the *F* center, it is necessary to consider two excited states, the 2*s*-like and 2*p*-like states.[14,51,52]

In the calculation of the probability of spontaneous emission, the cube of the emitted photon energy appears. However, we omit the factor in the following description since we are interested in the NWP behavior. Hereafter, we use the term "luminescence spectrum" as the shape function of the emission band, which is defined as the emission intensity divided by the cube of the energy.

A. Transient spectrum from the 2*s*-like state

The transient hot luminescence spectrum reflecting the NWP dynamics on the 2*s*-like APES is derived as follows. According to Ref. 50, the transient hot luminescence spectrum $F_e(\Omega_2,\Omega_1;t)$ is described as (hereafter, we adopt the unit $\hbar=1$)

$$F_e(\Omega_2,\Omega_1;t) \propto \frac{\sqrt{2\pi}}{\tilde{D}(t)} \exp\left[-\frac{\{\Omega_2-\tilde{\epsilon}(t)\}^2}{2\tilde{D}(t)^2}\right], \tag{1}$$

where Ω_1 and Ω_2 are the incident photon energy and the emitted one, respectively. $\tilde{\epsilon}(t)$ and $\tilde{D}(t)$ are, respectively, the time-dependent Franck-Condon energy and the time-dependent spectral width of the hot luminescence, which are given by

$$\tilde{\epsilon}(t) = \epsilon - 2E_{\mathrm{LR}} + 2\int_{-\infty}^{\infty} d\omega J(\omega)\cos\,\omega t\left\{\omega^{-1} + \frac{\Omega_1-\epsilon}{2D^2}\right\}, \tag{2}$$

$$\tilde{D}(t)^2 = D^2 - \frac{1}{D^2}\left\{\int_{-\infty}^{\infty} d\omega J(\omega)\cos\,\omega t\right\}^2. \tag{3}$$

Here, ϵ is the electronic excitation energy, E_{LR} is the lattice relaxation energy given by $\int_{-\infty}^{\infty} d\omega\omega^{-1}J(\omega)$, and D is the width given by $D^2=\int_{-\infty}^{\infty} d\omega J(\omega)$, where $J(\omega)$ is the spectral density function, which will be defined later.

Considering the experimental condition of the near resonant excitation and the finite initial spectral width caused by the laser pulse width, $\tilde{\epsilon}(t)$ and $\tilde{D}(t)$ are modified as

$$\tilde{\epsilon}(t) = \epsilon - 2E_{\mathrm{LR}} + 2\int_{-\infty}^{\infty} d\omega\omega^{-1}J(\omega)\cos\,\omega t, \tag{4}$$

$$\tilde{D}(t)^2 = D_0^2 + D^2 - \frac{1}{D^2}\left\{\int_{-\infty}^{\infty} d\omega J(\omega)\cos\,\omega t\right\}^2, \tag{5}$$

where D_0 is the initial spectral width.

Note that

$$\lim_{t\to 0}\tilde{\epsilon}(t) = \epsilon, \tag{6}$$

$$\lim_{t\to 0}\frac{d}{dt}\tilde{\epsilon}(t) = 0, \tag{7}$$

$$\lim_{t\to\infty}\tilde{\epsilon}(t) = \epsilon - 2E_{\mathrm{LR}}, \tag{8}$$

$$\lim_{t\to 0}\tilde{D}(t) = D_0, \tag{9}$$

$$\lim_{t\to\infty}\tilde{D}(t) = \sqrt{D_0^2+D^2} \equiv D_\infty, \tag{10}$$

where D_∞ is the final spectral width of the hot luminescence.

The spectral density function $J(\omega)$ specifies the lattice relaxation dynamics due to the electron-phonon interaction, i.e., the NWP dynamics. Various forms are assumed for $J(\omega)$, e.g., $\omega^2\times$Lorentzian by Kusunoki,[47] $\omega^2\times$Gaussian by Hama and Aihara,[48,49] $\omega^2\times$ellipse by Kayanuma,[50] and $\omega\times$double Gaussian by Tomimoto *et al.*[28] The last one consists of the product of a linear term and two Gaussian terms with the same peak frequency and different widths. Based on this spectral density function, the damped NWP oscillations associated with the formation of self-trapped excitons in quasi-one-dimensional halogen bridged platinum complexes have been numerically reproduced.[28] We adopt the double Gaussian function and assume the Gaussian components to peak at ω_{local}=11.5 meV ($\simeq$2.78 THz), which is the

frequency of the A_{1g} local mode. The spectrum $J(\omega)$ in our calculation is given by

$$J(\omega)=\begin{cases} g_{\mathrm{local}}\omega_{\mathrm{local}}\left\{\dfrac{1-\alpha}{\sqrt{\pi}W_1}\omega\exp\left[-\dfrac{(\omega-\omega_{\mathrm{local}})^2}{(W_1)^2}\right]+\dfrac{\alpha}{\sqrt{\pi}W_2}\omega\exp\left[-\dfrac{(\omega-\omega_{\mathrm{local}})^2}{(W_2)^2}\right]\right\} & \text{for } 0\leqslant\omega \\ 0 & \text{for } \omega<0. \end{cases} \tag{11}$$

Here, g_{local} is the dimensionless coupling constant corresponding to the Huang-Rhys factor, W_1 and W_2 are the energy widths, and α is the weight of the contribution of the second component of $J(\omega)$. By setting W_1 to be larger than W_2, the first component of $J(\omega)$ contributes to the NWP damping, while the second component to the long-lasting NWP oscillation.

The values of the above-described parameters are determined as follows. The electronic excitation energy ϵ is assumed to be the same as the incident photon energy Ω_1 of 1.823 eV because of the near resonant excitation condition; this is equivalent to omitting the second term in the integrand of Eq. (2). The lattice relaxation energy E_{LR} is given by the electronic excitation energy and the peak of the shape function of the emission band, $E_{2s}=\epsilon-2E_{\mathrm{LR}}\simeq\Omega_1-2E_{\mathrm{LR}}$. By using $E_{2s}=0.804$ eV,[35] E_{LR} is calculated to be 0.510 eV. The coupling constant g_{local} is given by $g_{\mathrm{local}}=E_{\mathrm{LR}}/\omega_{\mathrm{local}}=44$. The initial spectral width of the hot luminescence D_0 reflects the spectral width of the excitation pulse, $D_0\sqrt{8\ln 2}$ (FWHM) $=26.8$ meV, where $D_0=11.4$ meV. When D_0, g_{local}, and ω_{local} are determined, the final spectral width D_∞ is uniquely derived through Eq. (10) to be 77 meV because D is given by $D^2=\int_{-\infty}^{\infty}d\omega J(\omega)=g_{\mathrm{local}}\omega_{\mathrm{local}}$.[2] The narrower width of the spectral density function W_2 is assumed to be the spectral width of the A_{1g}-mode peak, 0.074 meV, in the resonance Raman spectrum.[37] The broader width W_1 is chosen to be 2.3 meV to reproduce the NWP damping. The 1.1 eV trace hardly shows the oscillatory wave form after several picoseconds, while the oscillation still lasts at 0.9 eV. In order to reproduce this feature, the parameter α is chosen to be 0.023. The value of $\alpha g_{\mathrm{local}}$ ($\simeq 1$) corresponds to the number of the vibrational sublevels related to the long-lived NWP. This means that the long-lived NWP is formed by the superposition of $n=0$ and 1 vibrational sublevels.

These parameters are listed in Table I. The obtained $J(\omega)$, $\tilde{\epsilon}(t)$, and $\tilde{D}(t)$ are plotted in Figs. 5(b), 6(a), and 6(b), respectively.

The lifetime of the $2s$-like excited state is determined by the radiative decay of 2.22 μs.[15] Since this value is much larger than the time range of 5 ps we are interested in, the radiative decay is ignored in the calculation.

B. Transient spectrum from the $2p$-like state

The transient hot luminescence spectrum reflecting the NWP dynamics on the $2p$-like APES, $f_e(\Omega_2,\Omega_1;t)$, is phenomenologically described below. We assume that the vibrational excited states in the $2p$-like state lose the coherence very quickly and obey the Boltzmann distribution. The validity of this assumption is described in Sec. IV.

The cooling of the Boltzmann distribution is reflected in the temporal evolution of the luminescence. The transient hot luminescence spectrum $f_e(\Omega_2,\Omega_1;t)$ is expressed as

$$f_e(\Omega_2,\Omega_1;t)\propto\sqrt{\frac{\pi}{\beta k_B T^*(t)}}\exp\left[-\frac{(\Omega_2-E_{2p})^2}{4\beta k_B T^*(t)}\right], \tag{12}$$

where E_{2p} is the peak energy of the $2p$-like emission, β is the constant with a dimension of energy corresponding to the lattice relaxation energy, and k_B is the Boltzmann constant. Here, the effective temperature $T^*(t)$ is introduced to include the effect of zero-point vibration correctly. The effective temperature $T^*(t)$ is given by

$$k_B T^*(t)=\frac{1}{2}\bar{\omega}\coth\left[\frac{1}{2}\frac{\bar{\omega}}{k_B T(t)}\right], \tag{13}$$

where $\bar{\omega}$ is the representative energy of the interaction modes for the $2p$-like state and $T(t)$ is the temperature of the relevant system which we assume to be

$$T(t)=T_\infty+(T_0-T_\infty)\exp[-t/\tau]. \tag{14}$$

Here, T_0 and T_∞ are the initial and final temperatures, respectively, and τ is the time constant of the cooling.

The values of these parameters are determined as follows. The peak energy of the $2p$-like emission E_{2p} is supposed to

TABLE I. Values of parameters in the model calculation of the time-resolved spectrum in the $2s$-like state $F_e(\Omega_2,\Omega_1;t)$. ϵ is the electronic excitation energy. E_{LR} is the lattice relaxation energy. D_0 and D_∞ are the initial and final spectral widths of hot luminescence. ω_{local} is the energy of the A_{1g} local mode. g_{local} is the dimensionless coupling constant. W_1 and W_2 are the energy widths of the first and second Gaussian components. α is the weight of the second component. In the second column, the notation "Fixed (Free)" means that the parameter is fixed (freely chosen) in the calculation.

Parameters	Fixed/Free	Values
ϵ (eV)	Fixed	1.823
E_{LR} (eV)	Fixed	0.510
D_0 (meV)	Fixed	11.4
D_∞ (meV)	Fixed	77
ω_{local} (meV)	Fixed	11.5
g_{local}	Fixed	44
W_1 (meV)	Free	2.3
W_2 (meV)	Fixed	0.074
α	Free	0.023

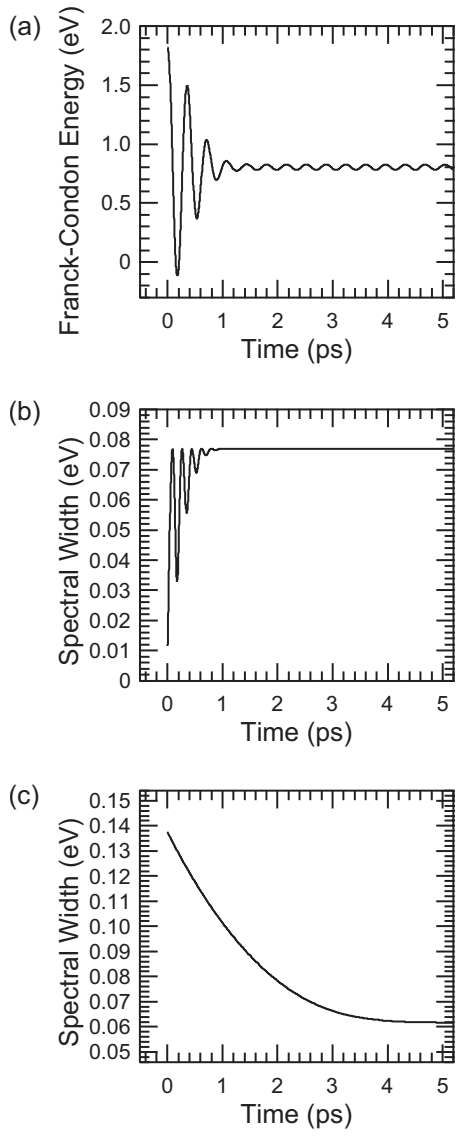

FIG. 6. (a) Time-dependent Franck-Condon energy on the $2s$-like APES $\tilde{\epsilon}(t)$. (b) Time-dependent spectral width of the hot luminescence from the $2s$-like state $\tilde{D}(t)$. (c) Time-dependent spectral width of the hot luminescence from the $2p$-like state $\sqrt{2\beta k_B T^*(t)}$.

be the same as that of the $2s$-like emission E_{2s} because the difference between E_{2s} and E_{2p} is 41.17 meV,[12] which is smaller than the energy resolution of our experimental system. The constant β is given by $\beta=(\Omega_1-E_{2p})/2=0.510$ eV. The final temperature T_∞ is assumed to be the bulk temperature of the sample, 10 K. After 4 ps, the width of the observed luminescence spectrum hardly varies, indicating that the system becomes cooled to the bulk temperature by that time. Namely, the temperature $T(t)$ approaches the final temperature T_∞ for $t>4$ ps. We assume that the instantaneous luminescence from the $2s$-like state is much weaker than that from the $2p$-like state (described later), so that the observed spectral width after 4 ps is reproduced by adjusting the final spectral width $\sqrt{(8\ln 2)2\beta k_B T^*(\infty)}$ (FWHM). Then the energy $\bar{\omega}$ is chosen to be 7.5 meV. Considering the above assumption, the spectral width at the time origin is also reproduced by adjusting the initial spectral width. The initial temperature T_0 is chosen to be 2.1×10^2 K. The time constant τ is determined to be 1.5 ps by fitting the overall traces of the 0.8 and 0.9 eV luminescences. These parameters are listed in Table II. The time dependence of the spectral width $\sqrt{2\beta k_B T^*(t)}$ is plotted in Fig. 6(c).

TABLE II. Values of parameters in the model calculation of the time-resolved spectrum in the $2p$-like state $f_e(\Omega_2,\Omega_1;t)$. E_{2p} is the peak energy of the shape function of the $2p$-like emission band. β is the constant. $\bar{\omega}$ is the representative energy of the interaction modes for the $2p$-like state. T_0 and T_∞ are the initial and final temperatures. τ is the time constant of the vibrational relaxation. In the second column, the notation "Fixed (Free)" means that the parameter is fixed (freely chosen) in the calculation.

Parameters	Fixed/Free	Values
E_{2p} (eV)	Fixed	0.804
β (eV)	Fixed	0.510
$\bar{\omega}$ (meV)	Free	7.5
T_0 (K)	Free	2.1×10^2
T_∞ (K)	Fixed	10
τ (ps)	Free	1.5

Since the radiative decay time of the $2p$-like excited state is expected to be about 2.7×10^{-8} s,[53] the exponential decay can be ignored in the calculation. We also ignore the nonradiative decay to the lower $2s$-like state.

C. Total spectrum

The total transient luminescence spectrum $F_e^{\rm tot}(\Omega_2,\Omega_1;t)$ is given by the linear combination of $F_e(\Omega_2,\Omega_1;t)$ and $f_e(\Omega_2,\Omega_1;t)$. The latter function is multiplied by 83 as the weighting factor due to the ratio of the oscillator strengths between the $2p$-like and $2s$-like states.[53] The total transient luminescence spectrum is expressed as

$$F_e^{\rm tot}(\Omega_2,\Omega_1;t)\propto(1-\gamma)F_e(\Omega_2,\Omega_1;t)+83\gamma f_e(\Omega_2,\Omega_1;t). \tag{15}$$

Here, γ is the diabatic transition probability from the $2s$-like state to the $2p$-like state during the NWP propagation through the anticrossing regions. In order to fit the experimental data, γ is chosen to be 0.05.

Finally, calculated curves are obtained by convolution of this spectrum function with the experimental response function, which has the Gaussian form with the width corresponding to the time resolution of the experimental system of 110 fs.

D. Calculation results

The calculated temporal evolutions of luminescence intensities at 0.8 and 0.9 eV are shown in Fig. 7 together with the experimental results. The circles represent the experimental data. The luminescence intensities are divided by the cube of their luminescence photon energies Ω_2.[3] The solid,

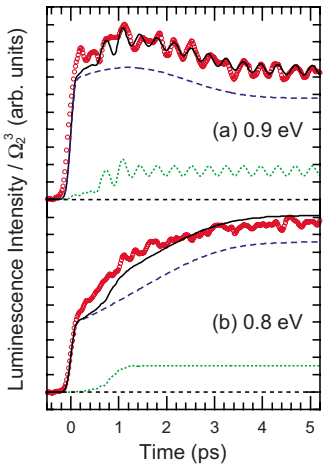

FIG. 7. (Color online) Time evolutions of luminescence intensities at 0.8 and 0.9 eV. The circles represent the experimental data. The luminescence intensities are divided by the cube of their luminescence photon energies $\Omega_2{}^3$. The solid, dashed, and dotted lines are the results of calculation of the total luminescence intensity $F_e^{\mathrm{tot}}(\Omega_2,\Omega_1;t)$, the luminescence from the $2p$-like APES $83\gamma f_e(\Omega_2,\Omega_1;t)$ (nonoscillatory component), and that from the $2s$-like APES $(1-\gamma)F_e(\Omega_2,\Omega_1;t)$ (oscillatory component), respectively. The intensities of the calculated curves are adjusted to overlap the experimental results for a convenient comparison.

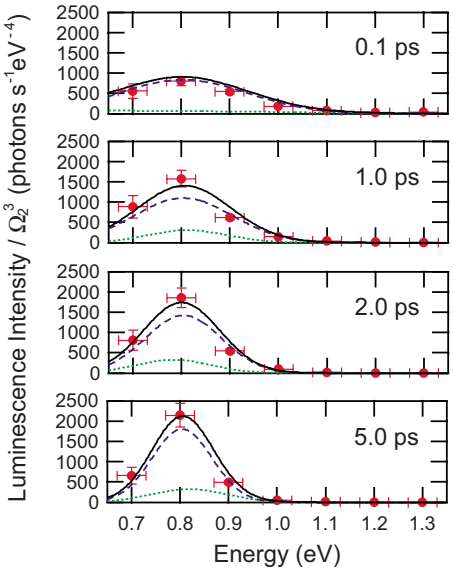

FIG. 8. (Color online) Time-resolved luminescence spectra at 0.1, 1.0, 2.0, and 5.0 ps. The ordinate shows the luminescence intensity divided by the cube of the luminescence photon energy $\Omega_2{}^3$. The meanings of symbols and lines are the same as in Fig. 7. The error bars in the ordinate indicate the measurement errors due to standard deviations of spectral sensitivities at respective energies. The error bars in the abscissa express the spectral resolution.

dashed, and dotted lines show the numerical results of the total luminescence $F_e^{\mathrm{tot}}(\Omega_2,\Omega_1;t)$, the contribution from the $2p$-like state $83\gamma f_e(\Omega_2,\Omega_1;t)$, and that from the $2s$-like state $(1-\gamma)F_e(\Omega_2,\Omega_1;t)$, respectively. Here, $83\gamma f_e(\Omega_2,\Omega_1;t)$ and $(1-\gamma)F_e(\Omega_2,\Omega_1;t)$ are convoluted with the instrumental function in the same manner as $F_e^{\mathrm{tot}}(\Omega_2,\Omega_1;t)$. In Fig. 7(a), the calculation reproduces the important features of the 0.9 eV trace: the fast rising around the time origin, the gradual rise until ~1 ps, the following decay, and the long-lasting oscillatory component with the low but constant visibility. In Fig. 7(b), the calculated result at 0.8 eV exhibits the kink around 0.1 ps and the following gradual increase.

The above-described features are explained below. The NWP, which adiabatically propagates to the $2s$-like state with the low oscillator strength, consists of the gap-mode-like A_{1g} local mode and oscillates over the detected time range. In contrast, the NWP transferred to the $2p$-like state quickly turns to be an incoherent vibrational population due to the very fast dephasing process and experiences the cooling due to another slower dephasing mechanism. (Details are described in Sec. IV.)

The time evolutions in the early time region especially within 1 ps cannot be correctly reproduced because we assume the spectral density function in the $2s$-like state $J(\omega)$ to have only one mode [Eq. (11)]. In the case that $J(\omega)$ has several peaks, the motion of the NWP is complex, which leads to the complicated time evolution of the luminescence intensity.[33]

The calculated time-resolved luminescence spectra at 0.1, 1.0, 2.0, and 5.0 ps are shown in Fig. 8 with the experimental results (circles). The spectrum at 0.1 ps indicates that the luminescence structure (nonoscillatory component) already exists around the peak of the stationary luminescence in the early stage of the lattice relaxation within the time resolution. This feature indicates that the incoherent distribution is generated in the $2p$-like state in such an early time. A series of the transient spectra represents that the spectral shape becomes narrow in accordance with the cooling process on the $2p$-like APES.

IV. DISCUSSION

The experimental results indicate the following two remarkable features: (1) There is a fast-rising broad structure with large intensity around the emission peak, 0.8 eV (Figs. 7 and 8). As time goes on, the spectral width of this structure becomes narrow, but the peak position does not move (Fig. 8). (2) Besides this large nonoscillatory component, the oscillation signal is seen in the temporal evolution of the luminescence intensity (Fig. 3). As described in Sec. II B, the oscillatory and nonoscillatory components originate from different luminescent states. These features suggest that the incoherent population is generated at a very early time on the APES which is different from the APES where the NWP oscillates, and also suggest that the incoherent population contributes to the large luminescence intensity. This is explained by the following NWP dynamics.

First, we consider the vibrational modes excited in absorption. Since the F center belongs to the cubic symmetry O_h, the A_{1g}, E_{1g}, and T_{2g} modes are allowed when the trapped electron is optically excited from $1s$ to $2p$ state. (When the spin-orbit interaction is taken into account, the coupling to the T_{1g} mode is involved.) These modes include

local modes as well as bulk phonon modes; the former means the lattice vibrations of six alkali ions around the vacancy, and the latter means the vibrations which spherically propagate from the F center. Under the experimental condition that the polarization of the excitation pulse is parallel to [100] crystal axis, the A_{1g} and E_{1g} modes are excited.

After being created in the FCS by optical absorption, the NWP slides down to the potential minimum. When the NWP passes through the anticrossing region on the lower APES [Fig. 1(c)], a large part adiabatically propagates on the lower APES (solid arrow), while a small fraction diabatically transfers to the upper APES (dashed arrow). Since the coupling of the trapped electron to the lattice vibrations depends on the electronic wave function, each NWP propagates along respective interaction modes and experiences the different vibrational relaxation process.

The $2s$-like APES has almost the $2s$ nature around the potential minimum; the fraction of the $2p$ component is about 1/83.[53] Because the $2s$ wave function is compact and isotropic, the $2s$ electron couples strongly to the totally symmetric local mode, i.e., the A_{1g} local mode. This is reflected in the Fourier power spectrum in Fig. 5(a), which has a large contribution of the A_{1g} local mode. Therefore, the NWP on the $2s$-like APES propagates along the interaction mode composed mainly of the A_{1g} local mode.

According to Ref. 38, in a KI crystal at 95 K, the upper limit frequency of the acoustic phonon branch is 2.06 THz [LA(L) phonon], and the lower and upper limit frequencies of the optical phonon branch are 2.93 THz [TO(L) phonon] and 4.26 THz [LO(Γ) phonon], respectively. The DOS spectrum shows the wide gap of ~0.87 THz between the acoustic and the optical phonon branch. Since the frequency of the A_{1g} local mode lies slightly below the lower limit of the optical phonon frequencies, the A_{1g} local mode will have a character of a gap mode. Thus, it is hardly scattered by bulk phonons, and the oscillation lasts for a long time. In fact, the resonance Raman scattering spectrum shows a very sharp A_{1g}-mode peak at 2.89 THz with a width of ~0.03 THz;[37] the expected lifetime of the A_{1g}-mode oscillation will be approximately $1/0.03 \simeq 30$ ps.

On the other hand, the $2p$-like APES almost has the $2p$ nature. Theoretical works suggest that the $2p$ wave function is spread with its maximum at four to five times the alkali-halogen distance[54] or more.[55] Therefore, the $2p$ electron interacts with bulk phonon modes of a wide range in the Brillouin zone more strongly than the $2s$ electron, and the interaction with the local modes will be ineffective. Consequently, the NWP on the $2p$-like APES experiences the relaxation along the interaction modes consisting of many bulk phonon modes with broad structures.

Bulk A_{1g} and E_{1g} modes are involved in both acoustic and optical phonon branches; that is, there are acoustic A_{1g}, optical A_{1g}, acoustic E_{1g}, and optical E_{1g} modes. One interaction mode will be formed by collecting the bulk phonon modes with the same symmetry in one phonon branch. Thus, four interaction modes couple to the $2p$-like electron.

The phase relationship within the interaction mode is intrinsically lost due to the finite width of the phonon spectrum[8] (we call here the "intrinsic dephasing"). As the spectral width of the interaction mode increases, the dephasing occurs faster.[56] The total spectral density is a sum of those of the four interaction modes, i.e., the spectral density of the total interaction mode, which is effectively wide enough to induce fast dephasing. Thus, the NWP on the $2p$-like APES can be regarded as an incoherent population in the early stage of the vibrational relaxation (about a few hundred femtoseconds or less). Since the probability amplitude corresponding to the incoherent superposition of vibrational wave functions fully extends on the $2p$-like APES, the broad luminescence spectrum appears in the early time region.

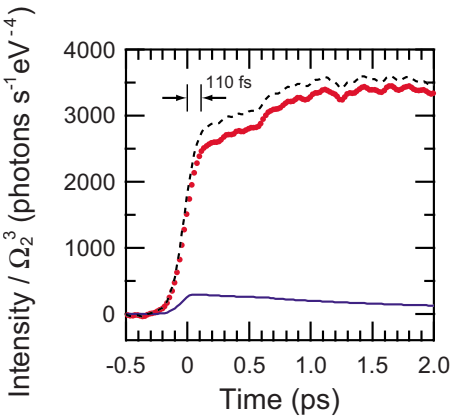

FIG. 9. (Color online) Temporal evolutions of the sum luminescence intensities. The circles represent the luminescence intensity [divided by the factor Ω_2^3] summed up from 0.7 to 1.3 eV. The solid line represents the mean value of the luminescence intensity summed up from 1.0 to 1.3 eV. The dashed line is the sum of the circles and the solid line.

The intrinsic dephasing means the energy dissipation from the relevant system at the same time. In other words, the bulk phonons leave from the F center with their respective group velocities.[57] As further intrinsic dephasings within respective interaction modes proceed, the vibrational population becomes concentrated in the lowest level. When probed at a certain point slightly away from the potential minimum, the luminescence intensity increases at the beginning and then decreases. This behavior is reflected in a part of the small rising within ~1 ps and in the subsequent gentle decrease in the luminescence intensity of the nonoscillatory component in Fig. 7(a). The model calculation supports the discussion above.

Finally, we examine how many times the NWP reaches the anticrossing regions by tracking the temporal evolution of the total luminescence intensity. After the transition from the $2s$-like to the $2p$-like state, the total luminescence intensity is expected to increase largely since the oscillator strength of the $2p$-like state is 83 times higher than that of the $2s$-like state. Figure 9 shows the temporal evolution of the sum of the luminescence intensities. The circles represent the luminescence intensities summed up from 0.7 to 1.3 eV. In order to obtain the total luminescence intensity, it is necessary to estimate the time-resolved luminescence below 0.7 eV. Because the stationary luminescence spectrum has a symmetric shape with respect to the emission peak at ~0.8 eV,[35,36] the sum intensity above 0.9 eV is substituted

for the sum intensity below 0.7 eV. The expected time evolutions below 0.7 eV will have the antiphase oscillation compared to those above 0.9 eV, so that we use its mean value (solid line). The obtained total intensity is shown as the dashed line, which indicates a steep rising within the time resolution of 110 fs and a slight increase until ~1 ps, followed by a virtual plateau. This implies that most of the diabatic transition from the lower APES to the upper takes place within 110 fs (within the first swing of the NWP). The slight increase until about 1 ps is ascribed to a transition via the tail of the NWP, which can reach the anticrossing regions.

V. CONCLUSION

In this work, we studied the nuclear wave-packet dynamics in the excited state of KI *F* centers. The experimental results show that the temporal evolution of the luminescence intensity involves the oscillatory and the nonoscillatory component. The results indicate that the nuclear wave packet partly experiences diabatic transitions around the anticrossing regions in the nearly degenerate $2s$ and $2p$ states.

The oscillatory part reflects the coupling of the $2s$ electron to the lattice vibration around the *F* center. The oscillation of the nuclear wave packet consists mainly of the local breathing mode, the A_{1g} local mode. The A_{1g} local mode will have a character of a gap mode, so that the oscillation lasts over the detected time range of 5 ps.

The nonoscillatory part reflects the coupling of the lattice vibration with the $2p$ electron. The $2p$ electron, which is rather spread, interacts with the bulk phonon modes more strongly than the $2s$ electron. Because of a wide frequency range of the normal modes interacting with the $2p$ electron, the nuclear wave packet in the $2p$-like state immediately becomes the incoherent vibrational population.

The diabatic transition of the nuclear wave packet would be almost completed in the first swing of its oscillation. A quantitative discussion is made by performing the model calculation based on the resonant secondary radiation theory involving the two excited states. The calculation suggests that the transition probability is approximately 0.05.

ACKNOWLEDGMENTS

We would like to thank Yosuke Kayanuma of Osaka Prefecture University for valuable discussions. This work has been supported by a Grant-in-Aid for Scientific Research (A) from the Ministry of Education, Culture, Sports, Science and Technology of Japan.

[1] *Femtochemistry, Ultrafast Chemical and Physical Processes in Molecular Systems*, edited by M. Chergui (World Scientific, Singapore, 1996), Chap. X.
[2] K. S. Song and R. T. Williams, *Self-Trapped Excitons*, Springer Series in Solid-State Sciences Vol. 105 (Springer-Verlag, Berlin, 1993).
[3] Y. Siegal, E. N. Glezer, and E. Mazur, in *Femtosecond Chemistry*, edited by J. Manz and L. Wöste (VCH, Weinheim, 1995), Vol. 2, p. 581.
[4] *Photoinduced Phase Transitions*, edited by K. Nasu (World Scientific, Singapore, 2004).
[5] T. Dekorsy, G. C. Cho, and H. Kurz, in *Light Scattering in Solids VIII*, edited by M. Cardona and G. Güntherodt (Springer-Verlag, Berlin, 2000), Chap. 4, p. 169.
[6] S. Hunsche, K. Wienecke, T. Dekorsy, and H. Kurz, Phys. Rev. Lett. **75**, 1815 (1995).
[7] M. Hase, M. Kitajima, S. I. Nakashima, and K. Mizoguchi, Phys. Rev. Lett. **88**, 067401 (2002).
[8] Y. Toyozawa and M. Inoue, J. Phys. Soc. Jpn. **21**, 1663 (1966); see also Y. Toyozawa, *Optical Processes in Solids* (Cambridge University Press, Cambridge, 2003).
[9] M. C. M. O'Brien, J. Phys. C **5**, 2045 (1972).
[10] T. Koyama, Y. Takahashi, M. Nakajima, and T. Suemoto, J. Chem. Phys. **124**, 221104 (2006).
[11] U. M. Grassano, G. Margaritondo, and R. Rosei, Phys. Rev. B **2**, 3319 (1970).
[12] K. Imanaka, T. Iida, and H. Ohkura, J. Phys. Soc. Jpn. **43**, 519 (1977).
[13] L. D. Bogan and D. B. Fitchen, Phys. Rev. B **1**, 4122 (1970).
[14] N. Akiyama and S. Muramatsu, Phys. Rev. B **67**, 125115 (2003).
[15] This value is given by the empirical formula of the activation-type temperature dependence of the lifetime of the excited *F* center in KI, which is derived by Swank and Brown [R. K. Swank and F. C. Brown, Phys. Rev. Lett. **8**, 10 (1962); Phys. Rev. **130**, 34 (1963)].
[16] Y. Mori, R. Hattori, and H. Ohkura, J. Phys. Soc. Jpn. **51**, 2713 (1982).
[17] Y. Mori, H. Hanzawa, and H. Ohkura, J. Lumin. **38**, 159 (1987).
[18] Y. Mori and H. Ohkura, J. Phys. Chem. Solids **51**, 663 (1990).
[19] A. Nakamura, T. Sano, Y. Kondo, and M. Hirai, J. Phys. Soc. Jpn. **56**, 1603 (1987).
[20] N. Akiyama and H. Ohkura, J. Lumin. **60&61**, 713 (1994).
[21] N. Akiyama, S. Muramatsu, S. Ide, and H. Ohkura, J. Lumin. **87-89**, 568 (2000).
[22] N. Akiyama, S. Muramatsu, and A. Tsuchihashi, J. Phys. Soc. Jpn. **70**, 1417 (2001).
[23] F. De Matteis, M. Leblans, W. Joosen, and D. Schoemaker, Phys. Rev. B **45**, 10377 (1992).
[24] F. De Matteis, M. Leblans, W. Slootmans, and D. Schoemaker, Phys. Rev. B **50**, 13186 (1994).
[25] M. Nisoli, S. De Silvestri, O. Svelto, R. Scholz, R. Fanciulli, V. Pellegrini, F. Beltram, and F. Bassani, Phys. Rev. Lett. **77**, 3463 (1996).
[26] R. Scholz, M. Schreiber, F. Bassani, M. Nisoli, S. De Silvestri, and O. Svelto, Phys. Rev. B **56**, 1179 (1997).
[27] S. Tomimoto, S. Saito, T. Suemoto, K. Sakata, J. Takeda, and S. Kurita, Phys. Rev. B **60**, 7961 (1999).
[28] S. Tomimoto, S. Saito, T. Suemoto, J. Takeda, and S. Kurita, Phys. Rev. B **66**, 155112 (2002).
[29] T. Matsuoka, J. Takeda, S. Kurita, and T. Suemoto, Phys. Rev.

Lett. **91**, 247402 (2003).
[30] T. Suemoto, T. Matsuoka, J. Takeda, and S. Kurita, J. Lumin. **108**, 167 (2004).
[31] Y. Takahashi and T. Suemoto, Phys. Rev. B **70**, 081101(R) (2004).
[32] T. Koyama, Y. Takahashi, M. Nakajima, and T. Suemoto, Phys. Rev. B **73**, 161102(R) (2006).
[33] K. Yasukawa, Y. Takahashi, S. Kurita, and T. Suemoto, Solid State Commun. **140**, 197 (2006).
[34] C. Z. van Doorn, Rev. Sci. Instrum. **32**, 755 (1961).
[35] These values are given by the empirical formulas of the temperature dependence of the absorption peak and width, which are derived by Gebhardt and Kühnert [W. Gebhardt and H. Kühnert, Phys. Status Solidi **14**, 157 (1966)]. The peak energy and width of the emission band are given likewise.
[36] W. Gebhardt and H. Kühnert, Phys. Lett. **11**, 15 (1964).
[37] D. S. Pan and F. Luty, in *Light Scattering in Solids*, edited by M. Balkanski, R. C. Leite, and S. P. Porto (Flammarion, Paris, 1976), p. 539.
[38] G. Dolling, R. A. Cowley, C. Schittenhelm, and I. M. Thorson, Phys. Rev. **147**, 577 (1966).
[39] In our preceding paper (Ref. 10), the Fourier power spectrum is calculated for the oscillating signal over 11 ps, and it has a relatively little contribution of bulk phonon modes. This is because the A_{1g} local mode causes the long-lasting NWP oscillation, so that this mode has a higher contribution in Fig. 4 of Ref. 10 than in Fig. 5 of the present paper.
[40] M. Gühr, M. Bargheer, and N. Schwentner, Phys. Rev. Lett. **91**, 085504 (2003).
[41] M. Gühr and N. Schwentner, Phys. Chem. Chem. Phys. **7**, 760 (2005).
[42] M. Fushitani, N. Schwentner, M. Schröder, and O. Kühn, J. Chem. Phys. **124**, 024505 (2006).
[43] V. Hizhnyakov and I. Tehver, Phys. Status Solidi **21**, 755 (1967).
[44] V. V. Hizhnyakov and I. J. Tehver, J. Lumin. **18/19**, 673 (1979).
[45] Y. Toyozawa, J. Phys. Soc. Jpn. **41**, 400 (1976).
[46] Y. Toyozawa, A. Kotani, and A. Sumi, J. Phys. Soc. Jpn. **42**, 1495 (1977).
[47] M. Kusunoki, Prog. Theor. Phys. **60**, 71 (1978).
[48] M. Hama and M. Aihara, Phys. Rev. B **36**, 8181(R) (1987).
[49] M. Hama and M. Aihara, Phys. Rev. B **38**, 1221 (1988).
[50] Y. Kayanuma, J. Phys. Soc. Jpn. **57**, 292 (1988).
[51] S. Muramatsu and K. Nasu, J. Phys. C **18**, 3729 (1985).
[52] S. Muramatsu, M. Aihara, and K. Nasu, J. Phys. C **19**, 2585 (1986).
[53] The expected lifetime of the $2p$ state, which is indicated by the oscillator strength of absorption, is about 2.7×10^{-8} s. The measured lifetime for a spontaneous emission from the RES is 2.22 μs (Ref. 15) and is 83 times longer than the expected one.
[54] W. B. Fowler, Phys. Rev. **135**, A1725 (1964).
[55] R. F. Wood and U. Öpik, Phys. Rev. **179**, 783 (1969).
[56] For example, supposing that $J(\omega)$ is the Ohmic spectral density with an exponential cutoff, i.e., $J(\omega)\propto\omega\exp[-\omega/\omega_c]$ (ω_c is a cutoff frequency), which is frequently used in discussing dissipative systems, the time-dependent Franck-Condon energy exhibits an overdamping behavior. That is, the NWP damps within about a quarter of the oscillation period, and the population becomes established around the potential minimum.
[57] When the spatial size of the electronic wave function is δL, the electron interacts with the modes in the part of the phonon branch which extends over the order of the inverse of δL in the Brillouin zone. Assuming that the corresponding frequency dispersion of the part of the branch is $\delta\omega$, the group velocity of the modes is estimated to be $\delta L\delta\omega$. Therefore, it takes $\delta L/(\delta L\delta\omega)=(\delta\omega)^{-1}$ for the phonon wave packet to leave from the F center and decouple the electron. This is the time constant of energy dissipation and comparable to the dephasing time of the phonons.